5328 *Inorg. Chem.* **2009**, *48*, 5328–5337
DOI: 10.1021/ic900320h

Inorganic Chemistry
Article

Structures from Powders: Polynuclear Hg(II) Complexes Containing the Flexible Bisimidazolylmethane Ligand

Norberto Masciocchi,*,† Alessandro Figini Albisetti,‡ Angelo Sironi,‡ Claudio Pettinari,*,§ Corrado Di Nicola,§ and Riccardo Pettinari§

†*Dipartimento di Scienze Chimiche e Ambientali, Università dell'Insubria e CNISM, via Valleggio, 11, 22100 Como, Italy,* ‡*Dipartimento di Chimica Strutturale e Stereochimica Inorganica, Università di Milano, via Venezian, 21, 20133 Milano, Italy, and* §*Dipartimento di Scienze Chimiche, Università di Camerino, via S. Agostino 1, 62032 Camerino (MC), Italy*

Received February 17, 2009

Several polynuclear Hg(II) complexes containing the flexible ditopic bisimidazolylmethane ligand ($C_7H_8N_4$, bim) have been prepared by reaction of equimolar quantities of mercury salts (acetate, cyanide, thiocyanate, chloride, and iodide) in EtOH or acetonitrile solution. Their crystal and molecular structures were retrieved from laboratory powder diffraction data, and their thermal properties were fully characterized, including the determination of the thermal expansion coefficients and the related strain tensor using thermodiffractometric methods. $[Hg(bim)(CH_3COO)_2]_2$ consists of cyclic dimers with chelating acetates, while the $[Hg(bim)X_2]_n$ species (X = Cl, CN, SCN, and I) are one-dimensional polymers, with dangling X groups. A further complex of nominal $Hg_2(bim)Cl_2$ formulation was also prepared, but the complexity and nonideality of its powder diffraction traces prevented the determination of its main structural features.

Introduction

Over the past few years, we have been interested in the coordination chemistry of polydentate ligands possessing multiple donor sites. Starting from simple heteroaromatic anions, such as pyrazolate,[1] imidazolate,[2] and pyrimidinolate,[3] we further increased the complexity of the polytopic N-ligands employed in the formation of monomeric, oligomeric, and polymeric species. For example, our recent results of substituted triazines,[4,5] scorpionates,[6] and substituted heterocycles[7] have allowed us to prepare and characterize a number of functional species, ranging from catalytically active (soluble) oligomers[8] to extended solids capable of molecular sensing and recognition.[9] Recently, when the isolated material was not available as single crystals of suitable quality, the structural characterization was performed employing state-of-the-art powder diffraction methods coupled with ^{13}C cross polarization−magic angle spinning (CP-MAS) NMR spectroscopy.[10]

Over the past few years, bisimidazolylmethane (bim),[11] a ligand employed for the investigation of the biological allosteric effect in zinc-gable porphyrin complexes[12] and as an artificial receptor capable of binding anionic guests,[13] has been successfully used as a flexible divergent donor to construct coordination polymeric materials. Several Ag,[14] Mn,[15] Cd,[16] Zn,[17] Co,[18] and Li[19] monodimensional zigzag

*To whom correspondence should be addressed. E-mail: norberto.masciocchi@uninsubria.it (N.M.).

(1) See, for example: Cingolani, A.; Galli, S.; Masciocchi, N.; Pandolfo, L.; Pettinari, C.; Sironi, A. *J. Am. Chem. Soc.* **2005**, *127*, 6144–6145.
(2) See, for example: Masciocchi, N.; Bruni, S.; Cariati, E.; Cariati, F.; Galli, S.; Sironi, A. *Inorg. Chem.* **2001**, *40*, 5897.
(3) See, for example: Navarro, J. A. R.; Barea, E.; Rodriguez Dieguez, A.; Salas, J. M.; Ania, C. O.; Parra, J. B.; Masciocchi, N.; Galli, S.; Sironi, A. *J. Am. Chem. Soc.* **2008**, *130*, 3978–3984 and references therein.
(4) Casellas, H.; Gamez, P.; Reedijk, J.; Mutikainen, I.; Turpeinen, U.; Masciocchi, N.; Galli, S.; Sironi, A. *Inorg. Chem.* **2004**, *44*, 7918–7924.
(5) Casellas, H.; Roubeau, O.; Teat, S. J.; Masciocchi, N.; Galli, S.; Sironi, A.; Gamez, P.; Reedijk, J. *Inorg. Chem.* **2007**, *46*, 4583–4591.
(6) Pettinari, C. *Scorpionates II: The Chelating Borate Ligands*; Imperial College Press: London, 2008.
(7) Galli, S.; Masciocchi, N.; Cariati, E.; Sironi, A.; Barea, E.; Haj, M. A.; Navarro, J. A. R.; Salas, J. M. *Chem. Mater.* **2005**, *17*, 4815–4824.
(8) Ardizzoia, G. A.; Cenini, S.; La Monica, G.; Masciocchi, N.; Moret, M. *Inorg. Chem.* **1994**, *33*, 1458–1463.
(9) Galli, S.; Masciocchi, N.; Tagliabue, G.; Sironi, A.; Navarro, J. A. R.; Salas, J. M.; Mendez-Liñan, L.; Domingo, M.; Perez-Mendoza, M.; Barea, E. *Chem.—Eur. J.* **2008**, *14*, 9890–9901.
(10) Masciocchi, N.; Galli, S.; Alberti, E.; Sironi, A.; Di Nicola, C.; Pettinari, C.; Pandolfo, L. *Inorg. Chem.* **2006**, *45*, 9064–9074.
(11) (a) Claramunt, R. M.; Elguero, J.; Meco, T. *J. Heterocycl. Chem.* **1983**, *20*, 1245–1249. (b) Li, J. *Acta Crystallogr.* **2006**, *E62*, o1798–o1799.
(12) Tabushi, I.; Sasaki, T. *J. Am. Chem. Soc.* **1983**, *105*, 2901–2902.
(13) In, S.; Kang, J. *J. Inclusion Phenom. Macrocyclic Chem.* **2006**, *54*, 129–132.
(14) Jin, C.-M.; Lu, H.; Wu, L.-Y.; Huang, J. *Chem. Commun.* **2006**, 5039–5041.
(15) Jin, S.; Chen, W. *Inorg. Chim. Acta* **2007**, *360*, 3756–3764.
(16) Jin, S.; Chen, W.; Qiu, H. *Cryst. Growth Des.* **2007**, *7*, 2071–2079.
(17) Jin, S.; Wang, D.; Chen, W. *Inorg. Chem. Commun.* **2007**, *10*, 685–689.
(18) Jin, S.-W.; Chen, W.-Z. *Polyhedron* **2007**, *26*, 3074–3084.
(19) Hwang, I.-C.; Chandran, R. P.; Singh, N. J.; Khandelwal, M.; Thangadurai, T. D.; Lee, J.-W.; Chang, J. A.; Kim, K. S. *Inorg. Chem.* **2006**, *45*, 8062–8069.

Published on Web 05/06/2009

Scheme 1. Schematic Drawing of the bim Ligand, Highlighting the Flexible Torsional Angles Discussed in the Text

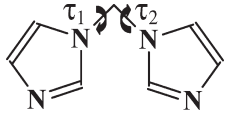

chains or two-dimensional grid network structures have been recently reported, and some of them have been described as promising candidates for application in electronic devices and catalysis. To date, no mercury derivatives of this ligand are known, notwithstanding a very recent report on the use of imidazolyl-based ligands for the preparation of luminescent polymeric mercury complexes, in which weak interactions play a significant role in the formation of supramolecular architectures.[20]

In particular, several oligomeric or polymeric species containing the neutral bisimidazolylmethane ligand (bim, see Scheme 1) have been recently prepared and studied by a combination of less-conventional structural methods;[21] these studies included a detailed analysis of the stereochemical preference about the two rotationally flexible CH_2-N bonds and the thermal characterization of the anisotropic thermal expansion coefficients and the thermal strain tensor derived therefrom.

We have now prepared several third-row transition metal derivatives (Hg(II) complexes), which were studied by X-ray powder diffraction (XRPD) methods and thermodiffractometry, adding a partial structural interpretation of the observed thermally induced deformations. Mercury compounds are extremely toxic, and it might appear somewhat unusual for researchers to systematically pursue their preparation, isolation, and full characterization. However, we found it very useful to determine the stereochemical preferences of Hg(II)-based bim-containing polymers, after we successfully addressed the nature, reactivity, and structure of several zinc and cadmium analogues in a very recent contribution.[21] In addition, in this particular case, the presence of a dominant scatterer makes it possible to accurately follow the trend of Hg···Hg interatomic distance changes upon thermal treatment, well beyond the typical accuracy normally granted by intrinsically poor (if compared with single-crystal) powder diffraction data.

Experimental Section

Materials and Methods. All reagents were obtained from commercial sources and were used without further purification. Solvents were distilled using the standard methods. The sample for microanalysis was dried in a vacuum to constant weight (293 K, ca. 0.1 Torr). Elemental analyses (C, H, N, S) were performed with a Fisons Instruments 1108 CHNS-O Elemental analyzer. IR spectra were recorded from 4000 to 600 cm^{-1} using a Perkin-Elmer Spectrum 100. Melting points (mp's) were undertaken with a SMP3 Stuart scientific instrument and in a capillary apparatus and were uncorrected. A Perkin-Elmer STA-6000 model thermogravimetric analyzer was used for determination of the thermal stabilities of mercury complexes. Samples weighing 5−10 mg were heated in a dynamic nitrogen atmosphere from 20 to 800 °C at a heating rate of 5 °C min^{-1}. The ligand bim has been prepared by standard literature methods.[22−24]

$[Hg(bim)(CH_3COO)_2]_2$, 1. An ethanol (20 mL) solution of bisimidazolylmethane (0.296 g, 2.0 mmol) was added to an ethanol (40 mL) solution of mercury(II) acetate, $Hg(OAc)_2$ (0.636 g, 2 mmol). A colorless precipitate formed. The suspension was stirred for 6 h and then was filtered off, and the colorless residue was washed with a mixture of ethanol/diethyl ether and identified as **1** (0.887 g, 95% yield). Elem anal. calcd for $C_{14}H_{14}HgN_4O_4$: C, 28.30; H, 3.02; N, 12.00. Found: C, 27.99; H, 2.93; N, 11.80. IR (KBr, cm^{-1}): 3114(m), 3024(w), 2935(m), 1559(s), 1523(m), 1504(m), 1391vs(vs), 1332m(vs), 1285(m), 1229(s), 1092(m), 1034(w), 1017(w), 944(w), 931(w), 859(w), 786(w), 764(m), 709(m) 666(s), 653(s), 618(m), 390(w).

$[Hg(bim)(SCN)_2]_n$, 2. An ethanol (20 mL) solution of bisimidazolylmethane (0.178 g, 1.2 mmol) was added to an ethanol (40 mL) suspension of mercury(II) thiocyanate, $Hg(SCN)_2$ (0.316 g, 1.0 mmol). A colorless precipitate immediately formed. The suspension was stirred for 6 h and then was filtered off, and the colorless residue was washed with 1:1 ethanol/diethyl ether (5 mL) and identified as **2** (0.348 g, 75% yield). Elem anal. calcd for $C_9H_8HgN_6S_2$: C, 23.25; H, 1.73; N, 18.08; S, 13.79. Found: C, 23.58; H, 1.69; N, 17.73; S, 13.93%. IR (cm^{-1}): 3121(m), 3025(w), 2113(s), 1521(m), 1499(m), 1441(w), 1419(w), 1386(m), 1229(s), 1188(w), 1117(m), 1085(s), 1025(w), 928(m), 847(m), 833(m), 750(s), 702(s). ^1H NMR (DMSO-d_6, 293 K): δ 6.35 (s, 2H, CH_{2Bim}), 7.03 (pd, 2H, CH_{Bim}), 7.57 (pt, 2H, CH_{Bim}), 8.18 (pd, 2H, CH_{Bim}).

$[Hg(bim)(CN)_2]_n$, 3. An acetonitrile (20 mL) solution of bisimidazolylmethane (0.075 g, 0.5 mmol) was added to an acetonitrile (40 mL) solution of mercury(II) cyanide, $Hg(CN)_2$ (0.126 g, 0.5 mmol). A colorless precipitate immediately formed. The suspension was stirred for 4 h and then was filtered off, and the colorless residue was washed by acetonitrile (5 mL) and identified as **4** (0.150 g, 75% yield). mp: 257 °C dec. Elem anal. calcd for $C_9H_8HgN_6$: C, 26.97; H, 2.01; N, 20.97. Found: C, 27.25; H, 1.95; N, 20.60%. IR (cm^{-1}): 3142(w), 3117(w), 3024(w), 1521(m), 1492(m), 1392(m), 1367(w), 1355(w), 1287(m), 1227(s), 1112(m), 1081(s), 1029(w), 921(m), 845(m), 771(m), 747(s), 708(s), 655(s). ^1H NMR (DMSO-d_6, 293 K): δ 6.33 (s, 2H, CH_{2Bim}), 7.00 (pd, 2H, CH_{Bim}), 7.52 (pt, 2H, CH_{Bim}), 8.16 (pd, 2H, CH_{Bim}).

$[Hg(bim)I_2]_n$, 4. An acetonitrile (20 mL) solution of bisimidazolylmethane (0.075 g, 0.5 mmol) was added to an acetonitrile (40 mL) solution of mercury(II) iodide, HgI_2 (0.224 g, 0.5 mmol). The red solution turned colorless in a few minutes, and then a colorless precipitate formed. The suspension was stirred for 6 h and was then filtered off, and the colorless residue was washed with acetonitrile (5 mL) and identified as **3** (0.280 g, 93% yield). mp: 206−208 °C dec. Elem anal. calcd for $C_7H_8I_2HgN_4$: C, 13.95; H, 1.34; N, 9.30. Found: C, 14.23; H, 1.28; N, 9.02%. IR (cm^{-1}): 3140(w), 3115(w), 3103(w), 3005(w), 1596(w br), 1521(m), 1504(m), 1486(m), 1386(m), 1280(m), 1232(m), 1111(m), 1093(s), 1084(s), 1022(m), 928(m), 8448m), 837(m), 771(m), 753(s), 738(s), 710(s), 652(s). ^1H NMR (DMSO-d_6, 293 K): δ 6.26 (s, 2H, CH_{2Bim}), 6.92 (pd, 2H, CH_{Bim}), 7.47 (pt, 2H, CH_{Bim}), 8.05 (pd, 2H, CH_{Bim}).

$[Hg(bim)Cl_2]_n$, 5. An acetonitrile (20 mL) solution of bisimidazolylmethane (0.178 g, 1.2 mmol) was added to an acetonitrile (40 mL) suspension of mercury(II) chloride, $HgCl_2$ (0.340 g, 1.1 mmol). A colorless precipitate formed.

(20) Wang, X.-F.; Yang, L.; Okamura, T.-A.; Kawaguchi, H.; Wu, G.; Sun, W.-Y.; Ueyama, N. *Cryst. Growth Des.* **2007**, *7*, 1125–1133.

(21) (a) Masciocchi, N.; Pettinari, C.; Alberti, E.; Pettinari, R.; Di Nicola, C.; Figini Albisetti, A.; Sironi, A. *Inorg. Chem.* **2007**, *46*, 10491–10500. (b) Masciocchi, N.; Pettinari, C.; Alberti, E.; Pettinari, R.; Di Nicola, C.; Figini Albisetti, A.; Sironi, A. *Inorg. Chem.* **2007**, *46*, 10501–10509.

(22) Lorenzotti, A.; Cecchi, P.; Pettinari, C.; Leonesi, D.; Bonati, F. *Gazz. Chim. Ital.* **1991**, *121*, 89–91.

(23) Pettinari, C.; Marchetti, F.; Lorenzotti, A.; Gioia Lobbia, G.; Leonesi, D.; Cingolani, A. *Gazz. Chim. Ital.* **1994**, *124*, 51–55.

(24) Pettinari, C.; Santini, C.; Leonesi, D.; Cecchi, P. *Polyhedron* **1994**, *13*, 1553–1562.

The suspension was stirred for 6 h and then was then filtered off, and the colorless residue was washed with acetonitrile (10 mL) and identified as **5** (0.369 g, 80% yield). Elem anal. calcd for $C_7H_8HgN_4Cl_2$: C, 20.03; H, 1.92; N, 13.35. Found: C, 19.93; H, 1.87; N, 12.95. IR (cm^{-1}): 3117(m), 3011(w), 1499(br), 1388(m), 1354(w), 1276(m), 1227(s), 1196(w), 1188(w), 1109(m), 1084(s), 1032(w), 1022(w), 943(w), 936(w), 928(w), 852(m), 844(m), 832(m), 782(m), 761(s), 750(s), 707(s), 654(s). ^1H NMR (DMSO-d_6, 293 K): δ 6.28 (s, 2H, CH_{2Bim}), 6.94 (pd, 2H, CH_{Bim}), 7.48 (pt, 2H, CH_{Bim}), 8.07 (pd, 2H, CH_{Bim}).

$[Hg_2(bim)Cl_2]_x$, 6. An acetonitrile (20 mL) solution of bisimidazolylmethane (0.178 g, 1.2 mmol) was added to an acetonitrile (40 mL) suspension of mercury(I) chloride, Hg_2Cl_2 (0.236 g, 0.5 mmol). A colorless precipitate formed. The suspension was stirred for 1 h and was then filtered off, and the colorless residue was washed with acetonitrile (10 mL) and identified as **6** (0.280 g, 90% yield). Elem anal. calcd for $C_7H_8Hg_2N_4Cl_2$: C, 13.56; H, 1.30; N, 9.03. Found: C, 13.86; H, 1.30; N, 8.87. IR (cm^{-1}): 3143(w), 3117(m), 3017(w), 1526 (m), 1508(m), 1492(m), 1427(w), 1394(m), 1353(w), 1285(m), 1229(s), 1196(m), 1115(m), 1097(m), 1086(s), 1035(w), 1025(w), 935(m), 850(m), 845(m), 760(s), 744(s), 708(s).

$[Hg(bim)Cl_2]_x \cdot x$DMSO, 7. Reaction between **5** and 2 equiv of DMSO in CH_2Cl_2 yields a powder that has been identified as **5**·DMSO. Elem anal. calcd for $C_9H_{14}Cl_2HgN_4OS$: C, 21.72; H, 2.83; N, 11.26; Found: C, 21.77; H, 3.02; N, 11.55. IR (cm^{-1}): 3118(w), 2995(w) 2912(w)), 1530(w), 1507(w) 1309(w) 1290(w), 1234(m), 1092(br), 1043(s), 1017(s), 951(m), 931(m), 896(w), 852(w), 765(m), 746(m), 697(m) 667(m).

X-Ray Powder Diffraction Analysis. Powdered, microcrystalline samples of **1**−**5** were gently ground in an agate mortar, then deposited in the hollow of an aluminum sample holder (equipped with a zero-background plate). Diffraction data were collected with overnight scans (16 h long) in the 5−105° 2θ range on a Bruker AXS D8 Advance diffractometer, equipped with a linear position-sensitive Lynxeye detector, primary beam Soller slits, and Ni-filtered Cu Kα radiation (λ = 1.5418 Å), sampling interval (in continuous mode) $\Delta 2\theta$ = 0.02°; divergence slit, 1.0°; goniometer raidus, 300 mm; generator setting, 40 kV, 40 mA. A standard peak search, followed by indexing with TOPAS,[25] allowed the detection of the approximate unit cell parameters, later improved by LeBail refinements. Indexing figures of merit (M/GoF, falling in the 23−77 value range) can be found in Table 1. Space group determinations, performed using systematic extinction conditions, in conventional mode as well using a structureless full pattern profile match, indicated as probable space groups (later confirmed by successful structure solutions and refinements) $P2_1/n$ for **1**, $P2_1/c$ for **2**, $C2/c$ for **3**,[26] and $P2_1/m$ for **4** and **5**. Structure solutions were performed (with the simulated annealing technique, as implemented in TOPAS, using for bim a partially flexible, rigid, idealized model,[27] independent metal, and, where pertinent, halide ions, as well as rigid acetate, Hg(cyanide)$_2$, or thiocyanide groups). The final refinements were carried out with the Rietveld method, maintaining the rigid bodies described above and allowing the refinement of the torsion angles of the methylene−heterocyclic rings linkage. Peak shapes were defined by the fundamental parameters approach implemented in TOPAS, while the crystal size effect was modeled by a Lorentzian broadening. The background contribution to the total scattering was modeled by Chebyshev's polynomials with two to eight coefficients, depending of the nature of the trace below Bragg peaks. One refinable isotropic thermal parameter was assigned to the metal atom, augmented by 2.0 Å^2 for lighter atoms. A preferred orientation correction was introduced (in the March-Dollase formulation) along the [111] direction for compound **3**. The final Rietveld refinement plots are shown in Figure 1. Table 1 contains a summary of crystal data and data collection parameters and structural analysis.

Thermodiffractometric experiments were performed in the air from 25 °C up to the decomposition temperatures using a custom-made sample heater, assembled by Officina Elettrotecnica di Tenno, Ponte Arche, Italy. Diffractograms at different temperatures (in 20 °C steps) were recorded typically in the range 8−35° 2θ. Linear parametric[28] Le Bail refinements eventually afforded the "best" set of cell parameters at the different temperatures. Linear thermal expansion coefficients were then derived from $(1/x)(\partial x/\partial T)$ versus T plots (x being either a lattice parameter or the cell volume). Later, for each compound, we selected the cell data at two well-separated temperatures (typically, 25 °C and the last useful point before decomposition, falling in the 125−245 °C range) and computed the thermal strain tensor and its eigenvalues and eigenvectors, using a locally developed program based on Ohashi's algorithm.[29] Thermal strain tensors were visualized with WinTensor,[30] which produces a VRML three-dimensional surface to be displayed, together with the (properly oriented) whole crystal structure, with the CORTONA VRML client. Crystal structures VRML pictures produced with Accelrys DS Visualizer 2.0.

Results and Discussion

Synthesis and Spectroscopy. Complexes **1** and **2** were synthesized by mixing an equimolar quantity of the mercury salts and bim in ethanol at room temperature, whereas **3**−**5** were isolated as colorless precipitates from MeCN solutions. All complexes are stable at room temperature and highly insoluble in water and in alcoholic and chlorinated solvents. Compound **6** has been obtained by reacting Hg_2Cl_2 with excess bim. Derivatives **2**−**5** were found to be moderately soluble in DMSO, their oligomeric or polymeric nature being likely modified by DMSO solvation or coordination: for example, from a DMSO solution of **5**, $[HgCl_2(DMSO)_2]$[31] was always recovered in quantitative yield; at variance, when an equimolar quantity of DMSO was added to a CH_3OH suspension of **5**, the coordination polymer **5** was recovered unaltered. Finally, when 1 equiv of **5** was reacted with 2 equiv of DMSO, a new species was obtained,

(25) *TOPAS*, version 3.0; Bruker AXS: Karlsruhe, Germany, 2005.

(26) Acentric *Cc*, a proper subgroup of *C*2/*c*, was also considered as a possible candidate. The complexity of the structure of species **3** within such a description (requiring the introduction of stiff restraints in order to reach convergence to a chemically significant model) and the absence of a cristallochemical clue (suggesting that a centrosymmetric structure is not tolerable), together with the presence of a dominating scatterer (the Hg ion), makes it impossible to assess *from powder data only*, the significance of the agreement factor lowering observed upon doubling the number of free structural parameters; therefore, the centric model was eventually adopted, which we believe to be consistent with all chemical and crystallographic data in our hands.

(27) For compounds **1**, **2**, and **3**, the Cartesian coordinates of bim derived from literature data were used (CCDC code: EZESEH), optimized by molecular mechanics, using Tinker (http://dasher.wustl.edu/tinker/). In species **4** and **5**, where the bim ligand is bisected by mirror planes, we adopted the z-matrix formalism, defining regular pentagons (C−X, 1.343 Å; C−H, 0.950 Å) for the heterocyclic ring (with their correct atomic species), hinged about a methylene bridge (CH_2−N, 1.457 Å) of idealized tetradedral geometry.

(28) Stinton, G. W.; Evans, J. S. O. *J. Appl. Crystallogr.* **2007**, *40*, 87–95.

(29) Ohashi, Y. In *Comparative Crystal Chemistry*; Hazen, R. M., Finger, L. W., Eds.; Wiley: New York, **1982**; pp 92−102.

(30) Kaminsky, W. *Wintensor: Tensor-drawing and calculation tool for Windows 95/98/NT/2000/XP*; University of Washington: Seattle, WA.

(31) Jain, S. C.; Rivest, R. *Inorg. Chim. Acta* **1969**, *3*, 552–558. James, B. R.; Morris, R. H. *Spectrochim. Acta A* **1978**, *34A*, 577–582.

Table 1. Crystal Data and Refinement Details for the Compounds **1**−**5**

compound $[Hg(Bim)X_2]_n$	**1**, CH_3COO^-	**2**, SCN^-	**3**, CN^-	**4**, I^-	**5**, Cl^-
emp. form.	$C_{11}H_8Hg_2N_4O_4$	$C_9H_8HgN_6S_2$	$C_9H_8HgN_6$	$C_7H_8HgN_4I_2$	$C_7H_8HgN_4Cl_2$
fw, g mol^{-1}	460.80	464.94	400.79	602.56	419.66
cryst syst	monoclinic	monoclinic	monoclinic	monoclinic	monoclinic
space group, Z	$P2_1/n$, 4	$P2_1/c$, 4	$C2/c$, 8	$P2_1/m$, 2	$P2_1/m$, 2
a, Å	9.4490(2)	14.2249(3)	14.2670(2)	9.1194(2)	8.3477(2)
b, Å	15.0057(3)	11.0098(3)	11.9344(1)	9.4293(1)	9.4314(2)
c, Å	10.2300(2)	9.1580(2)	14.8441(2)	8.4101(1)	6.8644(2)
β, deg	96.409(2)	110.300(2)	65.787(1)	118.519(1)	90.765(2)
V, Å^3	1441.43(5)	1345.19(6)	2305.13(5)	635.43(2)	540.39(2)
ρ_{calcd}, g cm^{-3}	2.123	2.296	2.310	3.149	2.579
$F(000)$	856	864	1472	528	384
μ(Cu−Kα), cm^{-1}	193.4	233.70	251.3	596.5	298.3
diffractometer	Bruker D8	Bruker D8	Bruker D8	Bruker D8	Bruker D8
T, K	298(2)	298(2)	298(2)	298(2)	298(2)
2θ range, deg	5−105	5−105	5−105	5−105	5−105
indexing method	SVD	SVD	SVD	SVD	SVD
M/GoF	68.7	23.3	28.2	71.3	76.7
N_{data}	5001	5001	5001	5001	5001
N_{obsd}	1666	1554	1332	792	617
R_p, R_{wp}[a]	0.072, 0.096	0.050, 0.067	0.073, 0.095	0.045, 0.058	0.041, 0.053
R_{Bragg}[a]	7.547	2.823	8.426	3.814	2.765
χ^2[a]	16.522	5.816	15.106	7.296	7.032
V/Z, Å^3	360.4	336.3	288.1	317.7	270.2

[a] $R_p = \sum_i |y_{i,o} - y_{i,c}|/\sum_i |y_{i,o}|$. $R_{wp} = [\sum_i w_i(y_{i,o} - y_{i,c})^2/\sum_i w_i(y_{i,o})^2]^{1/2}$. $R_B = \sum_n |I_{n,o} - I_{n,c}|/\sum_n I_{n,o}$. $\chi^2 = \sum_i w_i(y_{i,o} - y_{i,c})^2/(N_{obsd} - N_{par})$, where $y_{i,o}$ and $y_{i,c}$ are the observed and calculated profile intensities, respectively, while $I_{n,o}$ and $I_{n,c}$ are the observed and calculated intensities. The summations run over i data points or n independent reflections. Statistical weights w_i are normally taken as $1/y_{i,o}$.

identified by elemental analysis and IR as **5·DMSO**, a compound analogous to the already known $[HgI_2(dpb)(DMSO)]_n$ polymer (dpb = 2,3-di-(4-pyridyl)-2,3-butanediol).[32] Differently, compound **1** is poorly soluble also in DMSO, in contrast with its molecular (dimeric) structure (*vide infra*). However, when a DMSO suspension of **1** was heated at 90 °C for 30 min, displacement of the bim ligand from the mercury coordination sphere was observed.

Our observations suggest that, at room temperature, only excess DMSO is able to disrupt the polymeric structure of **2**−**5**, interacting with the tetrahedral mercury centers and breaking the Hg−N coordination bonds, whereas it was unable to interact with the dinuclear species **1**, in which the mercury ions are in an approximately coordinatively saturated pseudo-octahedral environment. Apparently, bim possesses a greater coordinating ability toward Hg^{2+} with respect to DMSO. Accordingly, when an equimolar quantity of bim is added to a MeOH solution of $[HgCl_2(DMSO)_2]$, immediate precipitation of **5** is observed.

The NMR data in DMSO of compounds **2**−**5** are not significantly different from those of the free ligand bim, suggesting that the polynuclear chains are completely destroyed in DMSO solution. Interestingly, the ^{1}H NMR spectrum of a mixture containing an equimolar quantity of DMSO and species **5** ($CDCl_3$ solution) exhibits signals different from those found for the free bim in the same solvent, suggesting that under these conditions not all Hg−N bonds are lost. As anticipated, when a large excess of DMSO-d_6 is added to the $CDCl_3$ solution of **5**, then formation of the $Hg(DMSO)_2Cl_2$ species is observed. In addition, the ^{1}H NMR spectrum of a *suspension* of **1** in DMSO-d_6, recorded at 90 °C, shows only signals of free bim, further supporting our hypothesis.

It is worth noting that, differently from that observed in the case of the already reported zinc and cadmium derivatives,[21b] when Hg(II) ions are used in the starting materials, only species showing the 1:1 HgX_2/bim stoichiometry were isolated, independently of the metal-to-ligand ratio employed. As expected, **6** shows a different stoichiometry, being the only species containing Hg in a lower oxidation state.

The IR spectra of these solid species typically show several bands usually associated with the organic ligand: signals of weak and medium intensity at ca. 3000 cm^{-1} (C−H stretching modes) and other more intense bands between 1600 and 1500 cm^{-1} (typical of ring breathing) are present, shifted to lower frequency by about 15−20 cm^{-1} from the reference free ligand values.[22−24]

Somewhat more informative are the IR spectra of the thiocyanate and cyanide complexes **2** and **4**: the well-defined absorption found at ca. 2110 cm^{-1} and the weaker one at ca. 2176 cm^{-1} are typical of monodentate *S*-CN[33] and *C*N[34] coordination modes, respectively.

As for derivative **1**, it is generally accepted that it is possible to distinguish between ionic, monodentate, chelating bidentate, or bridging bidentate groups on the basis of the $\Delta = \nu_a(COO) - \nu_s(COO)$ value. On the basis of the observed Δ value of 170 cm^{-1}, a chelating bidentate acetate is here predicted.[35] We have in fact compared the spectrum of **1** with those of a number of mononuclear[36] and polynuclear[37] mercury(II) acetate complexes and

(32) Niu, Y.; Guo, X.; Liu, X.; Wang, Q.; Zhang, N.; Zhu, Y.; Hou, H.; Fan, Y. *J. Chem. Crystallogr.* **2006**, *36*, 643–646.

(33) Mahmoudi, G.; Morsali, A.; Zhu, L. G. *Polyhedron* **2007**, *26*, 2885–2893.

(34) Goel, R. G.; Henry, W. P.; Ogini, W. O. *Can. J. Chem.* **1979**, *57*, 762–766.

(35) Mahmoudi, G.; Morsali, A.; Hunter, A. D.; Zeller, M. *Inorg. Chim. Acta* **2007**, *360*, 3196–3202.

(36) Roberts, P. J.; Ferguson, G.; Goel, R. G.; Ogini, W. O.; Restivo, R. J. *J. Chem. Soc., Dalton Trans.* **1978**, 253–256.

(37) Morsali, A.; Zhu, L.-G. *Helv. Chim. Acta* **2006**, *89*, 81–93.

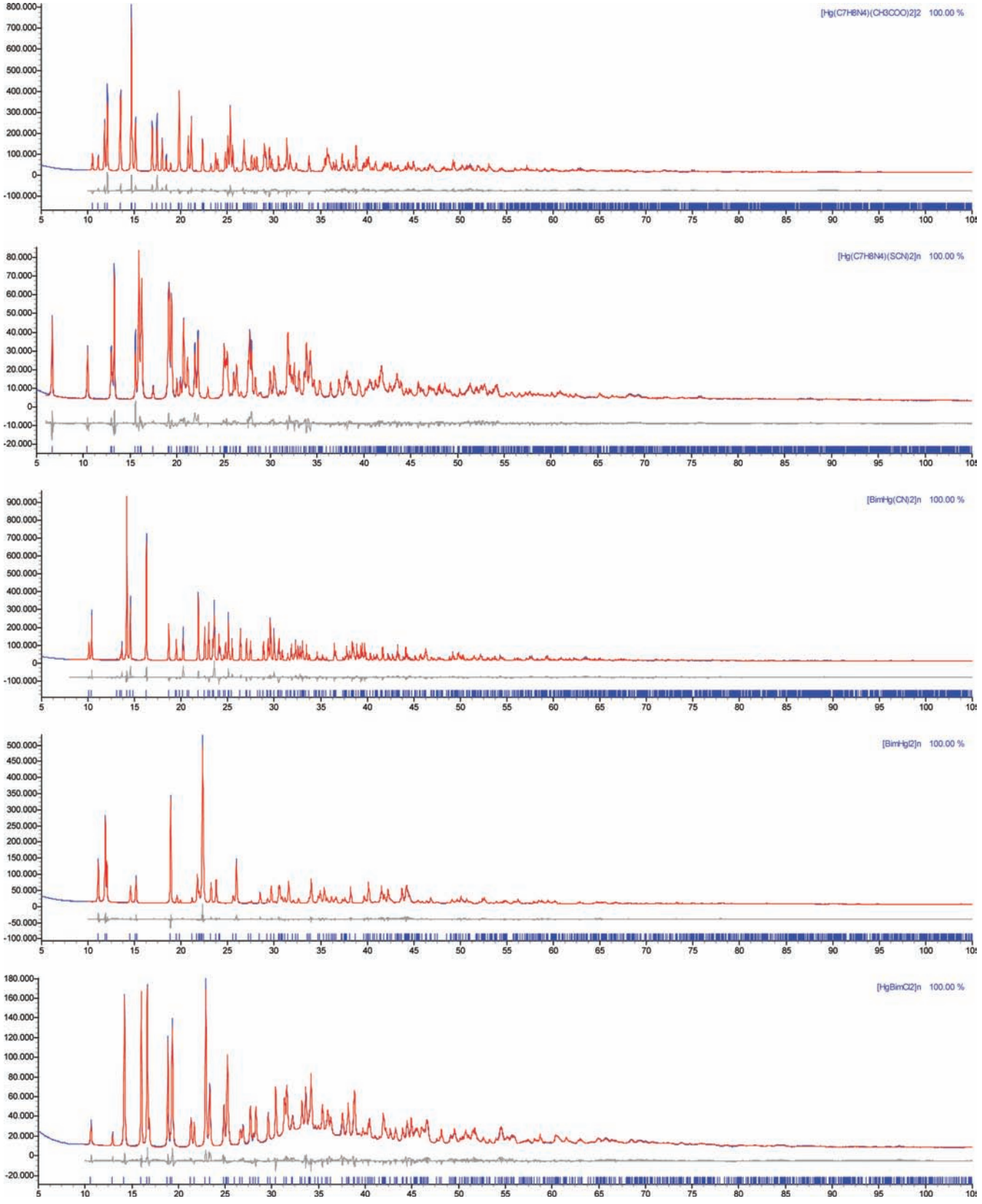

Figure 1. Rietveld refinement plots for compounds **1**−**5** with peak markers and difference plots at the bottom.

found that the spectrum of **1** shows strict similarity with spectra of $Hg(O_2CCH_3)_2(PR_3)_2$ species,[38] containing unsymmetrical chelating carboxylates. Chelating bidentate acetates normally have values of Δ less than 100 cm^{-1},[39] but this seems not to be applicable in the

(38) Alyea, E. C.; Dias, S. A. *Can. J. Chem.* **1979**, *57*, 83–90.

(39) Alcock, N. W.; Tracy, V. M.; Waddington, T. C. *J. Chem. Soc., Dalton Trans.* **1976**, 2243–2246.

case of $Hg(O_2CCH_3)_2$ complexes. In fact, the $Hg(O_2CCH_3)_2$ itself, for which two-coordination has been assigned, has a Δ value of 270 cm^{-1}, very different from the Δ found for **1**.[40]

Thermogravimetric Analysis. In order to examine the thermal stabilities of complexes **1**−**6**, thermal gravimetric analyses were carried out between 30 and 500 °C. The thermogravimetric analysis (TGA) curves for compounds **1**−**6** are supplied as Supporting Information, Figures S1−S6. Compound **1** is stable up to 144 °C, where it begins to decompose with a first exothermic effect. The observed weight loss (ca. 10.9%) has been assigned to the evolution of acetic anhydride and to the concomitant formation of a new species, which, on the basis of elemental analyses and IR spectroscopy, was formulated as $[Hg_2(bim)_2(CH_3COO)_2(O)]$. Indeed, the IR spectrum of the residue recovered after controlled heating at 200 °C exhibits a different absorption pattern in the 1700−1300 cm^{-1} region, suggesting a significant change in the coordination of the two residual acetates, which, in the heated material, likely act in the chelating or bridging chelating form. The second (complex) step of weight loss begins at ca. 255 °C and is complete at about 360 °C: a loss of acetic anhydride, sublimation of the organic ligand and Hg, and partial formation of a black residue (carbon), were observed. The thermal behavior of this compound is completely different from that reported for $[Hg(\mu\text{-}4,4'\text{-bipy})(\mu\text{-AcO})(AcO)]_n \cdot n/_2H_2O$, which shows two exothermic and one endothermic event up to 310 °C, finally forming HgO.[21]

The thiocyanate derivative **2** behaves in a different manner: after melting at ca. 164 °C, it starts to lose weight above 220 °C. At 300 °C, sublimation of the organic ligand is complete. The IR spectrum of the residue recovered after heating at 225 °C exhibits a signal corresponding to the SCN group, suggesting that at this temperature mercury thiocyanate is not decomposed to HgS. The solid residue formed at around 300 °C is the ligand-free $Hg(SCN)_2$, which is stable up to 390 °C and decomposes exothermically at higher temperatures. Species **3**, the cyanide analogue of **2**, is stable up to 239 °C, where it starts to release bim and Hg (up to 340 °C).

Interestingly, species **3**, $[Hg(bim)I_2]_n$, melts at ca. 210 °C and, at higher temperatures, completely decomposes into bim, molecular iodine, and Hg with a number of exothermic effects.[41] Slightly more interesting is the thermal behavior of the chloro-derivatives **5** and **6**. Indeed, **6** [a Hg(I) complex] is stable only below 100 °C, where is starts losing Hg and transforming to **5**, in agreement with the following disproportionation equation:

$$1/x[Hg_2(bim)Cl_2]_x \rightarrow 1/n[Hg(bim)Cl_2]_n + Hg$$

Above the transition temperature, the TG spectra of **5** and **6** are coincident; in particular, melting at ca. 250 °C, followed by the release of bim, elimination of the two chlorine atoms (likely as Cl_2), and then elimination of elemental Hg are observed.[42]

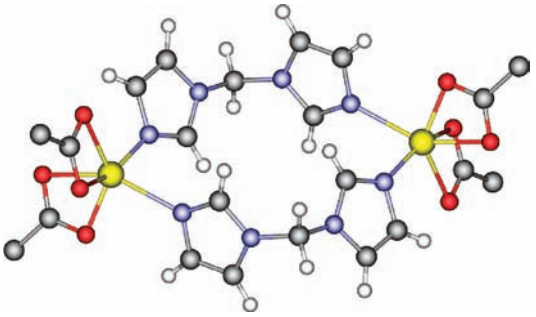

Figure 2. Schematic drawing of the structure of the $[Hg(bim)(CH_3COO)_2]_2$ (**1**) molecule, as derived by our powder diffraction analysis.

Structural Analysis. Our XRPD structure determination of **1** revealed the existence of cyclic, centrosymmetric dimers, crystallizing in the monoclinic $P2_1/n$ space group. In each dimeric molecule (shown in Figure 2), Hg(II) ions are hexacoordinated, thanks to the presence of two chelating acetates (Hg−O distances in the 2.22−2.32 Å range) and two nitrogen atoms from two different bim ligands (Hg−N distances 2.32−2.35 Å, restrained). The bim ligand bridges fairly distant Hg(II) ions, separated by 8.87 Å, thanks to the nearly C_s conformation induced by the two CH_2-im torsional angles. This conformation is not rare, as it has been already observed in oligomeric as well as polymeric metal complexes, both of the transition (Cu, Zn, Cd, Rh) or post-transition (Sn) type. Worthy of note, another common conformation, of ideal C_2 symmetry, has been observed and the relative geometric stereochemical preferences estimated on energetic grounds.

Similar cyclic oligomers have been found for zinc (another group 12 metal) and rhodium,[43] but not for cadmium complexes.[21b] Moreover, zinc dimers containing halides (Cl, Br) as ancillary ligands resulted to be very different from the corresponding acetate,[21b] which showed a one-dimensional chain topology (thus not crystallizing as discrete entities).

Our structural studies of **2**−**5** revealed that all of these species contain monodimensional chains determined by the juxtaposition of [−Hg−(bim)−] monomers, with the anionic ligands coordinated to the Hg(II) ions in a more-or-less ideal tetrahedral fashion. The most relevant geometrical features of the HgN_2X_2 chromophores are collected in Table 2, together with some ancillary stereochemical information. Schematic drawings of the infinite chains present in the $[Hg(bim)X_2]_n$ species are shown in Figure 3a−d.

Despite sharing a similar shape and conformation [the bim ligand is nearly—or exactly in **4** and **5**—C_s], several differences must be highlighted, both at the local coordination sphere of Hg(II) and at a supramolecular level. The dicyanide species **3** manifests the largest deviation from a tetrahedral coordination, with a (NC)Hg(CN) bond angle (>160°) approaching linearity. A similar coordination was found in mercury(II) bispyrazolate, with nearly linear N−Hg−N coordination and two significantly longer contacts in the plane normal to the

(40) Cooney, R. P. J.; Hall, J. R. *J. Inorg. Nucl. Chem.* **1972**, *34*, 1519.
(41) Mahmoudi, G.; Morsali, A.; Zeller, M. *Solid State Sci.* **2008**, *10*, 283–290.
(42) Popović, Z.; Soldin, Ž; Pavlović, G.; Matković-Čalogović, D.; Mrvoš-Sermek, D.; Rajić, M. *Struct. Chem.* **2002**, *13*, 425–436.
(43) Masciocchi, N.; Figini Albisetti, A.; Sironi, A.; Pettinari, C.; Marinelli, A. *Powder Diffr.* **2007**, *22*, 236–240.

Table 2. Synoptic Collection of Most Relevant Geometric Parameters (Å and deg) for Compounds **1**−**5**[a]

Compound	Hg···Hg	Hg−N	N−Hg−N	Hg-X	X-Hg-X	bim symmetry	1-D chain // to
1	8.87	2.32−2.35*	91.9	2.22−2.24, 2.30−2.32		C_s	
2	9.16	2.37*	91.7	2.42−2.43	135.3	C_s	[001]
3	9.30	2.40	96.1	2.05*	161.1	C_s	[110]
4	9.43	2.38	92.3	2.67−2.70	128.9	C_s	[010]
5	9.43	2.36	96.5	2.39−2.42	115.9	C_s	[010]

[a] Starred values (*) have been subjected to soft restraints.

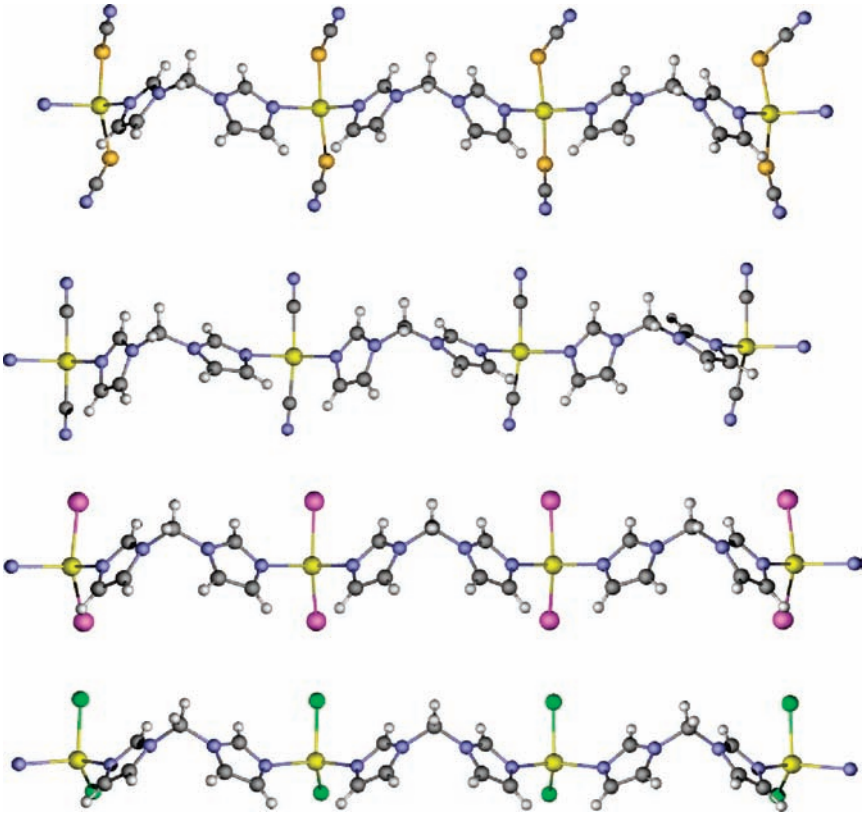

Figure 3. Schematic drawings of the structures of the $[Hg(C_7H_8N_4)(SCN)_2]_n$ (**2**), $[Hg(C_7H_8N_4)(CN)_2]_n$ (**3**), $[Hg(C_7H_8N_4)I_2]_n$ (**4**), and $[Hg(C_7H_8N_4)Cl_2]_n$ (**5**) molecules (top to bottom), as derived by our powder diffraction analysis.

N−Hg−N vector.[44] With the caveats imposed by the intrinsic low resolution of the method (particularly for the determination of light atoms in the presence of a heavy scatterer), it is however rewarding to see that the Hg−X trend nicely depends on the size of the ligand or that of the atom directly bound to the mercuric ion. Moreover, it should be noted that, no matter what the coordination of this ion is (pseudotetrahedral or nearly digonal with ancillary Hg−N contacts), N−Hg−N angles fall in a rather narrow range (92−97°), centered well below the ideal tetrahedral value of 109.5°.

Significant differences can also be found at the supramolecular level. This is particularly evident for the diiodide (**4**) and dichloride (**5**) couple, which in spite of sharing the same crystal system and space group (the not so common $P2_1/m$ one) when viewed down *b*, as shown in Figure 4, clearly manifest the different organization of adjacent chains.

Additionally, the cyanide and sulfocyanide couple also manifest significantly different crystal packings (not shown here), but this is much less surprising, since significant stereochemical differences are already present at the local level (*vide supra*). Perhaps, the most interesting supramolecular feature of compound **3** is the presence of crossed, but not weaved, polymeric chains running along [110] (and its symmetry equivalent direction, [−110]).

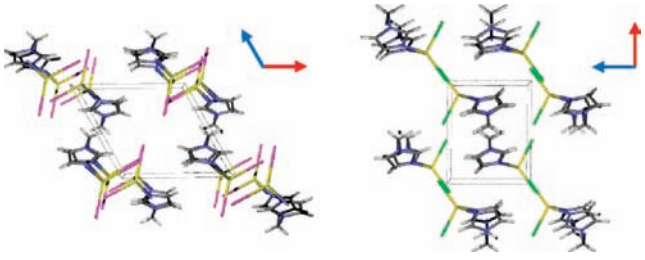

Figure 4. Schematic drawing of the crystal packing of $[Hg(C_7H_8N_4)I_2]_n$ (**4**) and $[Hg(C_7H_8N_4)Cl_2]_n$ (**5**) highlighting their nonisomorphic character (see text), *a* axis in red and *c* axis in blue.

Thermodiffractometric Analysis. Aiming at studying the dynamic behavior of these systems, we employed thermodiffractometric techniques to estimate the cell variations on increasing the temperature in "*in situ*"

(44) Masciocchi, N.; Ardizzoia, G. A.; La Monica, G.; Maspero, A.; Sironi, A. *Inorg. Chem.* **1999**, *38*, 3657–3664.

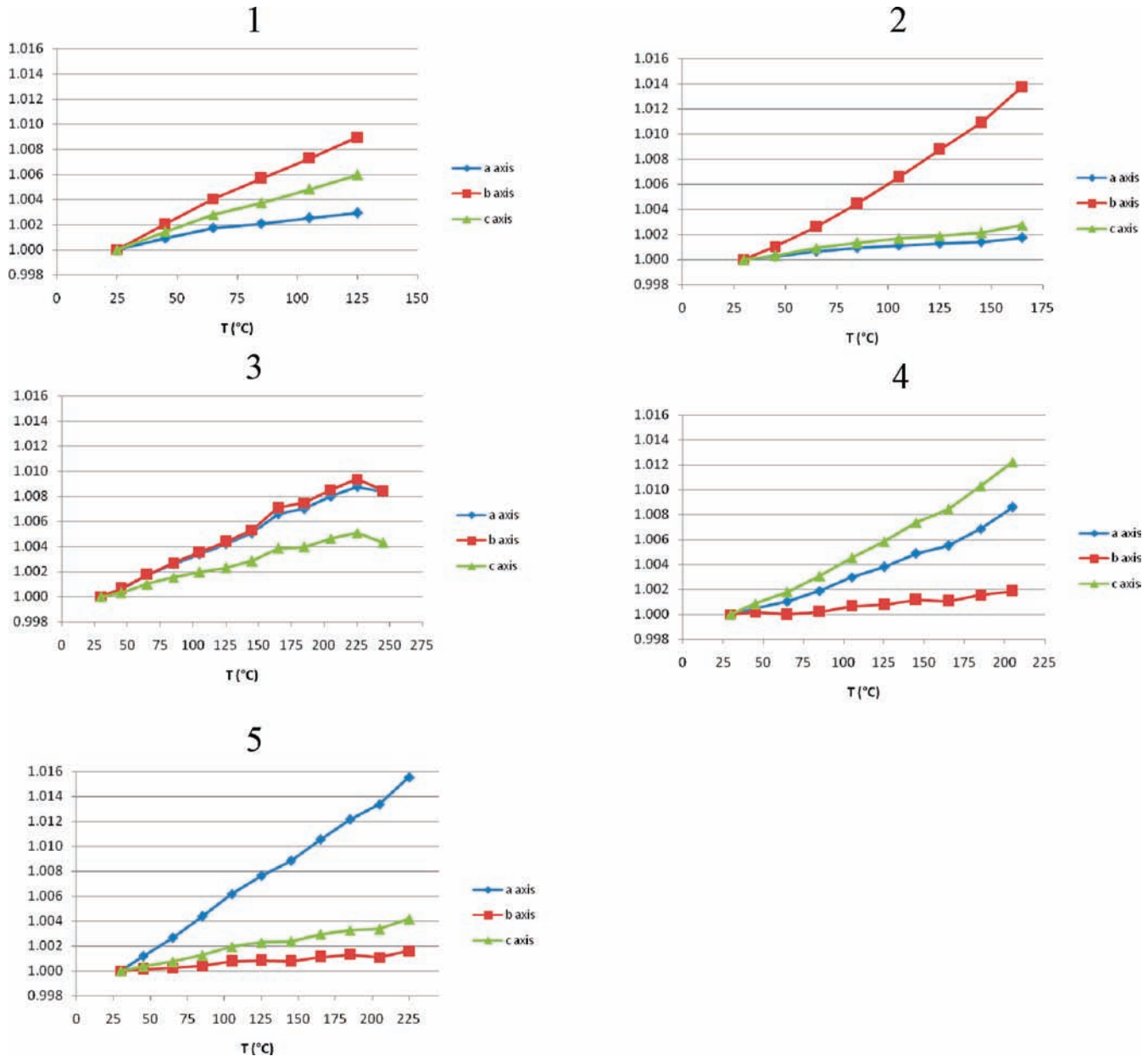

Figure 5. Temperature evolution of the lattice parameters of compounds **1**−**5**, normalized to their room temperature values.

experiments, using the anisotropic shifts of the diffraction peaks, and to build the corresponding strain tensor.[45] The numerically extracted results can be schematized as shown in Figure 5a−e, where the relative variations for the cell axes are plotted versus *T*. Figure 6a−e, instead, visualizes the thermal strain tensors, derived therefrom, positioned in the unit cell.

As can be observed in the plots of Figure 5, all cell axes increase with temperature, although at different rates. While this is a common behavior for intrinsically anisotropic molecular crystals, where most contacts are given by van der Waals interaction and are weak and, therefore, very sensitive to increased molecular motions (internal degrees of freedom, such as bond distances and angles being typically more rigid), in compounds **2** and **5**, there is one axis (*b* and *a*, respectively), which changes 5−10 times more than the others. However, simple axis deformations may be misleading when the lattice vectors are not orthogonal. In such cases, it is better to resort to strain tensors as represented by the anisotropic thermal expansion coefficient isosurfaces drawn in green in Figure 6a−e.

The deformation of a crystal by a change in the temperature is expected to be minimal in the direction of the highest atomic density, that is, the direction of strongest interactions; accordingly, all of the polymeric species (but **3**, *vide infra*) show small(er) thermal distortion along the chain elongation axis. At variance, the softer direction is that parallel to the vector bisecting the BIM N−C−N angle, which is substantially "perpendicular" to the pseudostacking of the imidazolyl rings (and to the chain elongation axis). This said, it is now clear why **3** has an "oblate" rather then a "prolate" strain tensor. Indeed, in **3** the *ab* plane contains both the chain elongation axes and the BIM N−C−N bisecting vectors of

(45) Zotov, N. *Acta Crystallogr.* **1990**, *A46*, 627–628.

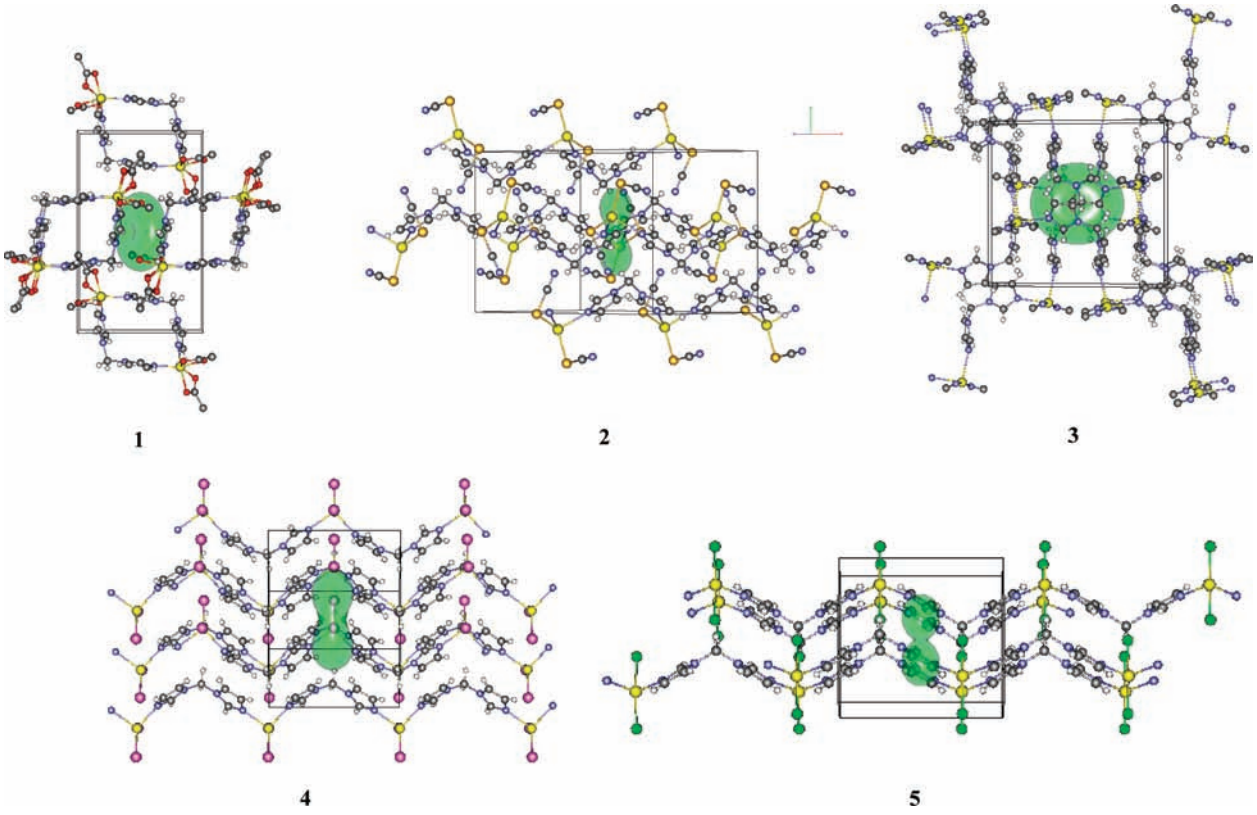

Figure 6. Thermal expansion coefficients' isosurface (thermal strain tensors) drawn within the crystal structure of compounds **1** (along *c*,*a* from left to right, *b* from bottom to top), **2** (the same orientation as for **1**), **3** (the same orientation as for **1**), **4** (along *b*,*a* from left to right, *c* from top to bottom), and **5** (along *b*,*a* from left to right and *c* from bottom to top).

the two crossed polymers. Thus, the hardest elongation direction of one polymer couples with the softest one of the other polymer, and this eventually explains why, in **3**, the polymeric chains are apparently aligned with the softer directions.

Further (less common) structural information was derived from structural refinements of the polymeric species on all collected XRPD data sets: thanks to the large contribution to the total scattering of the unique Hg ions, we derived the temperature dependence of the (bim-bridged) Hg···Hg distances, collectively shown in Figure 7. As shown therein, a large change, of nearly 0.10 Å, occurs for the cyanide derivative **3**, which is, after all, a definite outlier in our structural analysis, for it shows a nearly diagonal coordination and an unusual crystal packing with crossed polymeric chains. According to the explanation given above for the anomalous shape of the strain tensor, we must conclude that Hg···Hg elongation is here triggered by the lateral vibrations of the "orthogonal" crossed chains.

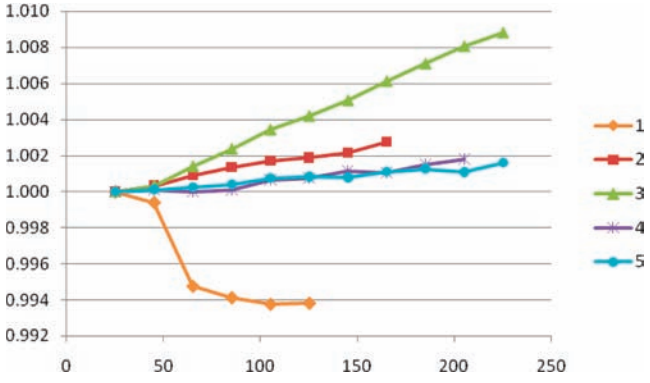

Figure 7. Temperature evolution of the intramolecular Hg···Hg distance in polymers **1**−**5**.

Conclusions

In summary, we have here presented the complete structural characterization of several novel mercury complexes (one cyclic dimer and several chain polymers) from powder diffraction data, together with some of the material performances derived from thermodiffractometric analysis, linking a structural interpretation with the (apparently incoherent) observed lattice deformation.

It is very interesting that, in contrast to other SCN, CN, and I complexes where the anions acted as bridges over adjacent metal ions (increasing structural dimensionality), in our cases, only chain polymers were obtained where the bridging linker is the N_2-donor ligand.

Our thermogravimetric studies demonstrated that, in the case of the halide and pseudohalide polymeric complexes, the interaction between the N_2-ligand and the mercury ion is weak, breaking of the Hg−N bonds with dissociation into the starting free ligand and mercury salts being observed in the temperature range 150−230 °C. On the other hand, these complexes, although not very stable on heating, were found to be rather resistant to solvent attack (with the notable, though expected, exception of DMSO). Work can be anticipated in the direction of studying the structure versatility of this system, for example, by employing different anions or synthetic conditions.

Acknowledgment. This work was supported by MUR (PRIN2006: "Materiali Ibridi Metallo-Organici Multifunzionali con Leganti Poliazotati") and Fondazione CARIPLO (Project 2007-5117). We gratefully acknowledge the help of one reviewer, which allowed us to make this paper, in its final version, more easily readable.

Supporting Information Available: TGA traces for compounds **1**−**6**, the tables of the lattice parameter evolution as obtained from Le Bail fits on selected portions of the XRPD trace, and the crystallographic data for compounds **1**−**5**. This material is available free of charge via the Internet at http://pubs.acs.org. CCDC 720632−720635 can be obtained free of charge from The Cambridge Crystallographic Data Centre via www.ccdc.cam.ac.uk/data_request/cif.